

Biophysical properties of voltage-gated Na⁺ channels in frog parathyroid cells and their modulation by cannabinoids

Yukio Okada^{1,*}, Kotapola G. Imendra⁴, Toshihiro Miyazaki², Hitoshi Hotokezaka³, Rie Fujiyama¹, Jorge L. Zeredo¹, Takenori Miyamoto⁵ and Kazuo Toda¹

¹*Integrative Sensory Physiology*, ²*Oral Cytology and Cell Biology* and ³*Orthodontics and Biomedical Engineering, Graduate School of Biomedical Sciences, Nagasaki University, Nagasaki, Nagasaki 852-8588, Japan*, ⁴*Department of Physiology, Faculty of Medicine, University of Ruhuna, Galle, Sri Lanka* and ⁵*Department of Chemical and Biological Sciences, Faculty of Science, Japan Women's University, Bunkyo-ku, Tokyo 112-8681, Japan*

*Author for correspondence (e-mail: okada@net.nagasaki-u.ac.jp)

Accepted 2 November 2005

Summary

The membrane properties of isolated frog parathyroid cells were studied using perforated and conventional whole-cell patch-clamp techniques. Frog parathyroid cells displayed transient inward currents in response to depolarizing pulses from a holding potential of -84 mV. We analyzed the biophysical properties of the inward currents. The inward currents disappeared by the replacement of external Na⁺ with NMDG⁺ and were reversibly inhibited by $3 \mu\text{mol l}^{-1}$ TTX, indicating that the currents occur through the TTX-sensitive voltage-gated Na⁺ channels. Current density elicited by a voltage step from -84 mV to -24 mV was -80 pA pF⁻¹ in perforated mode and -55 pA pF⁻¹ in conventional mode. Current density was decreased to -12 pA pF⁻¹ by internal GTP γ S (0.5 mmol l⁻¹), but not affected by internal GDP β S (1 mmol l⁻¹). The voltage of half-maximum ($V_{1/2}$)

activation was -46 mV in both perforated and conventional modes. $V_{1/2}$ of inactivation was -80 mV in perforated mode and -86 mV in conventional mode. Internal GTP γ S (0.5 mmol l⁻¹) shifted the $V_{1/2}$ for activation to -36 mV and for inactivation to -98 mV. A putative endocannabinoid, 2-arachidonoylglycerol ether (2-AG ether, $50 \mu\text{mol l}^{-1}$) and a cannabinomimetic aminoalkylindole, WIN 55,212-2 ($10 \mu\text{mol l}^{-1}$) also greatly reduced the Na⁺ current and shifted the $V_{1/2}$ for activation and inactivation. The results suggest that the Na⁺ currents in frog parathyroid cells can be modulated by cannabinoids *via* a G protein-dependent mechanism.

Key words: parathyroid, voltage-gated Na⁺ channel, G protein, activation, inactivation, cannabinoid, frog.

Introduction

Parathyroid hormone (PTH) regulates extracellular free Ca²⁺ concentration ($[\text{Ca}^{2+}]_o$) in cooperation with 1,25-dihydroxycholecalciferol (1,25(OH)₂D₃) and calcitonin (CT). On the other hand, $[\text{Ca}^{2+}]_o$ regulates the secretion of PTH from parathyroid cells through extracellular Ca²⁺-sensing receptor (CaR; Brown et al., 1993; Hofer and Brown, 2003). High $[\text{Ca}^{2+}]_o$ inhibits and low $[\text{Ca}^{2+}]_o$ enhances PTH secretion. It is believed that extracellular Ca²⁺ inhibits the secretion of PTH *via* the intracellular free Ca²⁺ concentration ($[\text{Ca}^{2+}]_i$). However, the molecular mechanism by which $[\text{Ca}^{2+}]_i$ regulates PTH secretion is not well elucidated.

Several electrophysiological studies have been performed in mammalian parathyroid cells. Those using classical intracellular microelectrodes indicated that rodent parathyroid cells display a deep resting potential (about -70 mV), which is depolarized by increasing $[\text{Ca}^{2+}]_o$ (Bruce and Anderson, 1979; López-Barneo and Armstrong, 1983). Later, the patch-clamp technique was applied on bovine, human and rodent

parathyroid cells (Castellano et al., 1987; Jia et al., 1988; Komwatana et al., 1994; Kanazirska et al., 1995; McHenry et al., 1998; Välimäki et al., 2003). These studies showed that parathyroid cells possess some types of K⁺ channels. Other studies suggested the presence of voltage-gated Ca²⁺ channels in bovine and goat parathyroid cells (Sand et al., 1981; Chang et al., 2001). However, voltage-gated Na⁺ channels could not be found in any of the aforementioned studies.

Ion channels are regulated by neurotransmitters and hormones *via* G protein-coupled receptors (GPCRs; Wickman and Clapham, 1995; Dascal, 2001). GPCRs dissociate heterotrimeric G proteins (G $\alpha\beta\gamma$) to G α -GTP and G $\beta\gamma$. Both subunits can regulate a variety of ion channels directly (*via* physical interactions between G protein subunits and the channel protein) or indirectly (*via* second messengers and protein kinases).

In the present study, we report that frog parathyroid cells possess voltage-gated Na⁺ channels and that their activity may be modulated by cannabinoids.

Materials and methods

Cell preparation

Adult bullfrogs *Rana catesbeiana* Shaw weighing 250–550 g were used for the experiment over the course of a year. Experiments were performed in accordance with the Guidelines for Animal Experimentation of Nagasaki University. Parathyroid cells were isolated from the parathyroid glands of decapitated and pithed animals. Two pairs of the oval parathyroid glands in both sides were quickly dissected from the pre-cardial region, where they lie near the ventral branchial bodies and attached to the carotid arteries (Sasayama and Oguro, 1974). The glands were cut into small pieces in Ca^{2+} -free saline containing 2 mmol l^{-1} EDTA and incubated for 12–15 min in 2 ml of the same saline containing 10 mmol l^{-1} L-cysteine and 10 units ml^{-1} papain (Sigma, St Louis, MO, USA). The glands were then rinsed with normal saline. The individual cells were dissociated by gentle trituration in normal saline. Isolated parathyroid cells displayed an oval-shape, with a diameter of about $10 \mu\text{m}$ (Fig. 1).

Electrophysiological recording

Voltage-clamp recording was performed in whole-cell configuration (Hamill et al., 1981) using a CEZ 2300 patch-clamp amplifier (Nihon Kohden, Tokyo, Japan). The patch pipettes were pulled from Pyrex glass capillaries containing a fine filament (Summit Medical, Tokyo, Japan), using a two-stage puller (Narishige PD-5, Tokyo, Japan). The tips of the electrodes were heat-polished with a microforge (Narishige MF-80). The resistance of the resulting patch electrode was 5–10 $\text{M}\Omega$ when filled with internal solution. The formation 5–20 $\text{G}\Omega$ seals between the patch pipette and the cell surface was facilitated by applying weak suction to the interior of the pipette. The patch membrane was broken by applying strong suction, resulting in a sudden increase in capacitance. Amphotericin B ($133\text{--}160 \mu\text{g ml}^{-1}$, Sigma) was added to the

pipette solution when using the perforated method (Rae et al., 1991). The perforated whole-cell condition was obtained within 5 min of the establishment of a $\text{G}\Omega$ seal. Recordings were made from parathyroid cells that had been allowed to settle on the bottom of a chamber placed on the stage of an inverted microscope (Olympus IMT-2, Tokyo, Japan). The recording pipette was positioned with a hydraulic micromanipulator (Narishige WR-88). The current signal was low-pass-filtered at 5 kHz, digitized at 125 kHz using a TL-1 interface (Axon Instruments, Union City, CA, USA), acquired at a sampling rate of 2–10 kHz using a computer running the pCLAMP 5.5 software (Axon Instruments), and stored on hard disk. The pCLAMP was also used to control the digital-analogue converter for the generation of the clamp protocol. The indifferent electrode was a chlorided silver wire. The voltages were corrected for the liquid junction potential (-4 mV) between normal saline solution and the standard K^+ internal solution. Capacitance and series resistance were compensated for, as appropriate. The series resistances after compensation in perforated mode were in the range 8–15 $\text{M}\Omega$. The whole-cell current–voltage (I – V) relationship was obtained from the current generated by the 70 ms voltage step pulses between -74 and $+56 \text{ mV}$ in 10 mV increments from a holding potential of -84 mV . The voltage-dependence of steady-state inactivation was studied in a conventional manner by applying stepwise 200 ms conditioning pulses over the range from -124 mV to -34 mV and a single depolarization to -34 mV near the peak of the I – V curve. The time course of recovery from inactivation was measured by double-pulse protocols. Input resistance was calculated from the slope conductance generated by the voltage ramp from -104 to -54 mV .

Data analysis

Data were analyzed with pCLAMP and Origin 7.5 (Origin Lab, Northampton, MA, USA). Unless stated otherwise, the data are presented as means \pm S.E.M., significance was tested by Student's t -test and a difference was considered significant if $P < 0.05$. The steady-state inactivation curves were fitted with a Boltzmann equation as follows:

$$I / I_{\max} = \{1 + \exp[(V - V_{1/2})/k]\}^{-1}, \quad (1)$$

where I/I_{\max} is the current magnitude normalized to its maximum value, V designates the conditioning voltage, $V_{1/2}$ is the voltage at which the magnitude is half-maximum, and k is a Boltzmann slope factor, which reflects the voltage sensitivity of steady-state inactivation of the current. The conductance for activation was estimated according to the following equation:

$$G = I / (V - V_{\text{rev}}), \quad (2)$$

where G is the peak conductance, I is the current magnitude at the test voltage (V), and V_{rev} is the apparent reversal potential for the Na^+ current. The activation curve was also fitted with the Boltzmann equation as follows:

$$G / G_{\max} = \{1 + \exp[(V - V_{1/2})/k]\}^{-1}, \quad (3)$$

where G/G_{\max} is the conductance magnitude normalized to its

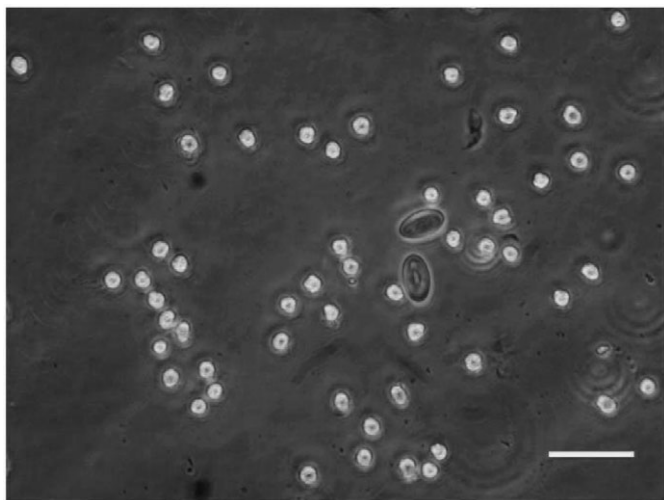


Fig. 1. Freshly isolated frog parathyroid cells are white and oval-shaped in this phase-contrast image. Two large cells in the center of the image are the erythrocytes. Bar, $50 \mu\text{m}$.

maximum value, V designates the test voltage, and other parameters are the same as above. Recovery from inactivation was fitted using:

$$I_{\text{test}} / I_{\text{control}} = a[1 - \exp(-t/\tau)], \quad (4)$$

where t is time, a is maximum magnitude, and τ is time constant for the recovery.

Solution and drugs

Normal saline solution consisted of (in mmol l^{-1}): NaCl 115, KCl 2.5, CaCl_2 1.8, HEPES 10; glucose 20, pH 7.2. The pH of normal saline and other solutions was adjusted by Tris base. The extracellular Na^+ -free solution was prepared by the replacement of Na^+ with NMDG $^+$. The solution exchange was done by gravity flow. For stock solution, tetrodotoxin (3 mmol l^{-1} ; Sigma), spermine tetrahydrochloride (100 mmol l^{-1} ; Sigma) and adrenaline bitartrate (10 mmol l^{-1} ; Sigma) were dissolved in deionized water. WIN 55,212-2 mesylate (10 mmol l^{-1} ; Tocris, Bristol, UK), phorbol 12,13-dibutyrate (PDBu, 10 mmol l^{-1} ; Sigma), forskolin (10 mmol l^{-1} ; Sigma) and chelerythrine chloride (10 mmol l^{-1} ; Sigma) were dissolved in dimethylsulphoxide (DMSO). 2-arachidonoylglycerol ether (2-AG ether, 13.7 mmol l^{-1}) dissolved in ethanol was purchased from Tocris. Samples of the stock solutions were added to normal saline solution to give the desired final concentrations.

The standard K^+ internal solution contained (in mmol l^{-1}): KCl 100, CaCl_2 0.1, MgCl_2 2, EGTA 1, HEPES 10, pH 7.2. GTP γ S (0.5 mmol l^{-1} , Sigma) and GDP β S (1 mmol l^{-1} , Sigma) were dissolved in the internal solution on every experimental day.

All experiments were carried out at room temperature ($20\text{--}25^\circ\text{C}$).

Results

Basal properties of isolated frog parathyroid cells

Under conventional whole-cell mode in a standard K^+ internal solution, frog parathyroid cells displayed resting potential of -10 to -70 mV ($-30 \pm 2 \text{ mV}$, $N=44$). The input resistance ranged from 4.7 to $25.0 \text{ G}\Omega$ ($13.7 \pm 0.9 \text{ G}\Omega$, $N=44$) and the membrane capacitance was $5.8\text{--}11.0 \text{ pF}$ ($7.6 \pm 0.2 \text{ pF}$, $N=44$). On the other hand, under perforated whole-cell mode using amphotericin B, the cell displayed resting potentials of -10 to -87 mV ($-26 \pm 3 \text{ mV}$, $N=26$). In perforated mode, the input resistance ranged from 4.5 to $50.0 \text{ G}\Omega$ ($11.1 \pm 1.8 \text{ G}\Omega$, $N=26$), and the membrane capacitance was $6.0\text{--}13.0 \text{ pF}$ ($7.9 \pm 0.4 \text{ pF}$, $N=26$). Differences in basal membrane properties were not significant between conventional and perforated conditions.

Activation

After attaining the perforated whole-cell configuration in normal saline solution, almost all frog parathyroid cells displayed transient inward currents in response to depolarizing voltage steps from a holding potential of -84 mV (Fig. 2A). Although the pipette contained a K^+ internal solution, leak currents, but not the voltage-gated outward current could be found. The threshold for the inward current activation ranged from -64 to -54 mV (Fig. 2B). The inward currents were activated more rapidly with successive depolarizing steps. The activation time reaching a peak at -24 mV , for instance, was $0.69 \pm 0.04 \text{ ms}$ ($N=27$). Removal of external Na^+ completely abolished the inward currents (3 cells; Fig. 3A), indicating that the currents were caused predominately by Na^+ . Application of $3 \mu\text{mol l}^{-1}$ TTX (a voltage-gated Na^+ channel blocker) totally eliminated the inward currents (8 cells; Fig. 3B) after about 4 min. The currents recovered to $92.2 \pm 12.2\%$ ($N=8$) of

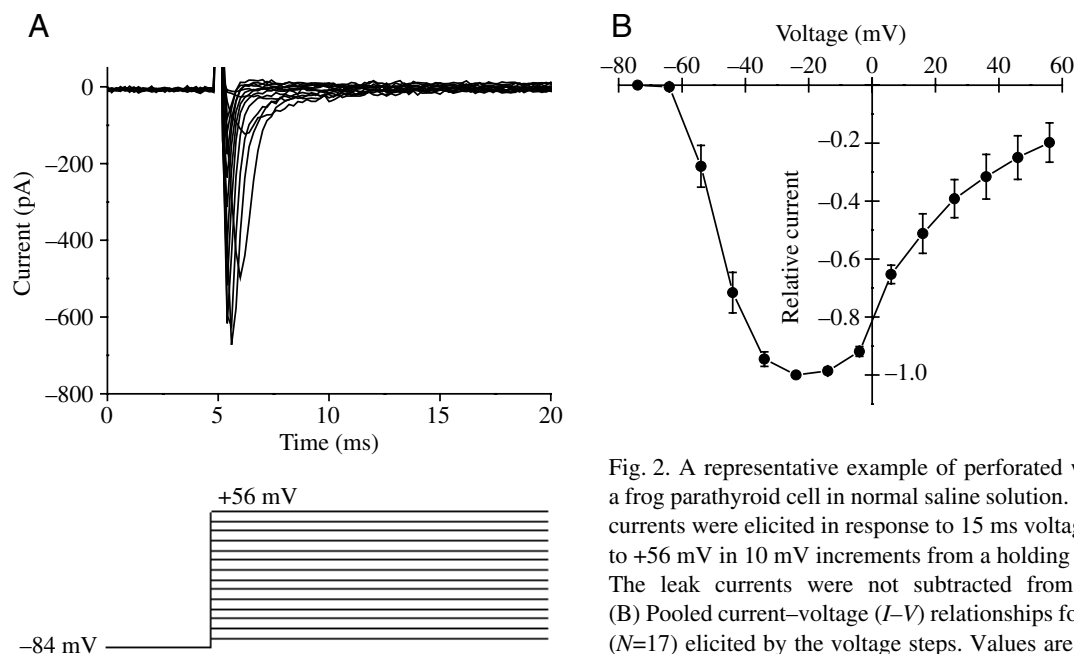


Fig. 2. A representative example of perforated whole-cell current of a frog parathyroid cell in normal saline solution. (A) Transient inward currents were elicited in response to 15 ms voltage steps between -74 to $+56 \text{ mV}$ in 10 mV increments from a holding potential of -84 mV . The leak currents were not subtracted from the current traces. (B) Pooled current-voltage (I - V) relationships for the inward currents ($N=17$) elicited by the voltage steps. Values are means \pm S.E.M.

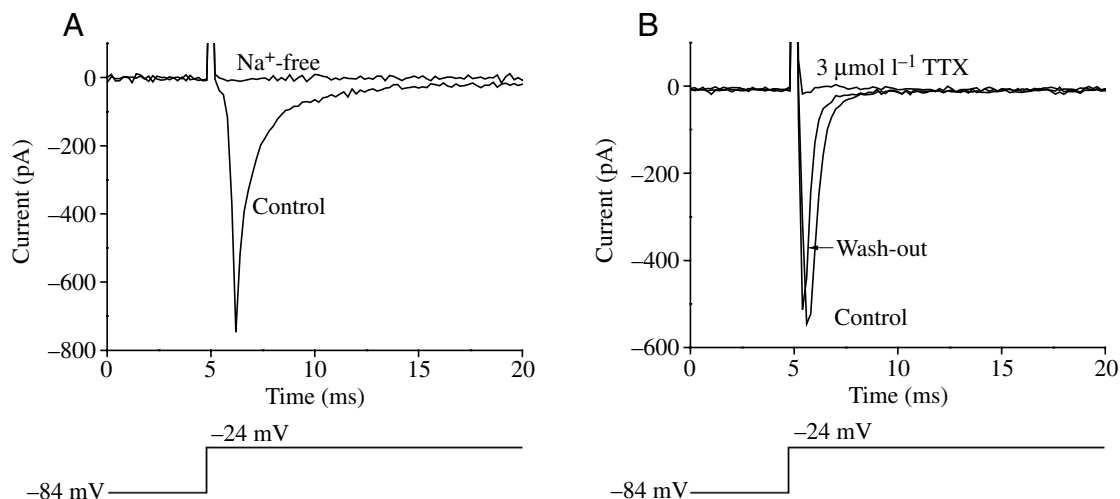


Fig. 3. Effects of the elimination of external Na⁺ (A) and the addition of 3 μmol l⁻¹ TTX to external normal saline solution (B) on the transient inward currents. The currents were elicited by 15 ms step pulses from a holding potential of -84 mV to a test potential of -24 mV.

the controls after about 10 min of washing with normal saline solution.

Membrane-delimited G protein-regulation of voltage-gated Na⁺ channels has been suggested. We also investigated the effect of GTPγS on the Na⁺ channels in frog parathyroid cells. Activation parameters were compared with each other in the presence and absence of GTPγS. Peak inward current elicited by a voltage step from -84 to -24 mV was -663±74 pA (*N*=27) in perforated mode, whereas the current decreased to -419±33 pA (*N*=30, *P*<0.05) in conventional mode. GDPβS (1 mmol l⁻¹) added to the intracellular solution did not affect the current amplitude (-413±88 pA, *N*=7) as compared with conventional mode, but internal 0.5 mmol l⁻¹ GTPγS significantly decreased the current to -93±10 pA (*N*=8, *P*<0.05). Similar results were observed for current density

(expressed as the ratio of current amplitude to cell capacitance). The magnitudes of the current density were -79.5±6.6 pA pF⁻¹ (*N*=27) in perforated mode, -55.2±4.4 pA pF⁻¹ (*N*=30) in conventional mode, -49.8±9.2 pA pF⁻¹ (*N*=7) in the condition containing 1 mmol l⁻¹ GDPβS and -11.6±1.3 pA pF⁻¹ (*N*=8) in the condition containing 0.5 mmol l⁻¹ GTPγS, respectively. The voltage of half-maximum activation *V*_{1/2} in perforated mode was estimated from the activation curve (*V*_{1/2} = -45.7±0.8 mV, *N*=17; Fig. 4A). The *V*_{1/2} in conventional mode (-46.1±1.1 mV, *N*=18) was almost the same. Addition of 1 mmol l⁻¹ GDPβS into the pipette solution did not change the *V*_{1/2} (-45.1±1.7 mV, *N*=6) as compared with conventional mode, but internal 0.5 mmol l⁻¹ GTPγS shifted the *V*_{1/2} to -35.5±3.3 mV (*N*=8, *P*<0.05; Fig. 4B).

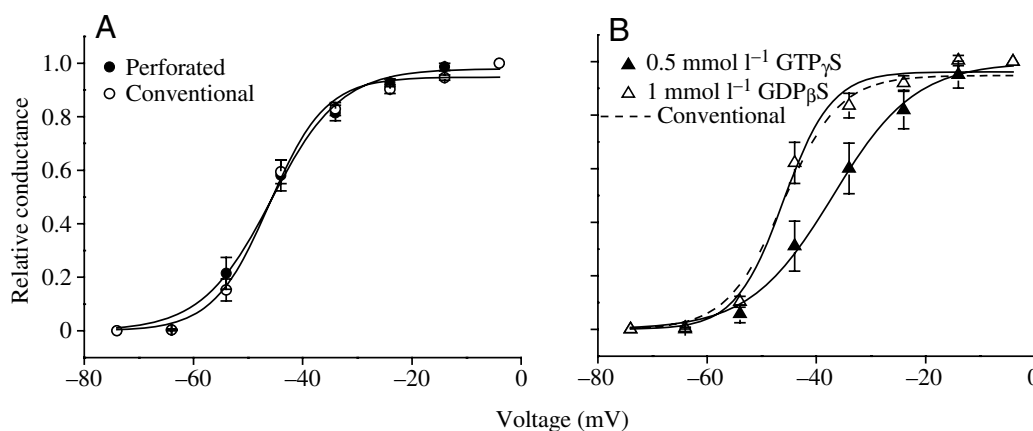


Fig. 4. Voltage dependence of activation of the Na⁺ currents, determined by *I*-*V* relationships for the Na⁺ currents elicited by the voltage steps. Smooth curves are simple Boltzmann functions. (A) *V*_{1/2} = -45.7 mV, *k* = -6.4 mV for perforated recording (filled circles), *V*_{1/2} = -46.1 mV, *k* = -5.2 mV for conventional recording (open circles). (B) *V*_{1/2} = -35.5 mV, *k* = -7.6 mV for 0.5 mmol l⁻¹ GTPγS (filled triangles), *V*_{1/2} = -45.1 mV, *k* = -4.4 mV for 1 mmol l⁻¹ GDPβS (open triangles). For comparison, the broken line for conventional recording is plotted in B. The values are means ± S.E.M. obtained from 6–18 cells.

Inactivation

We measured inactivation time constant (τ) for inactivation onset during a test pulse to -24 mV. The inactivation time constant in perforated mode (0.87 ± 0.08 ms, $N=27$) was shorter than the constant in conventional mode (1.13 ± 0.06 ms, $N=30$, $P < 0.05$). Internal 1 mmol l^{-1} GDP β S and 0.5 mmol l^{-1} GTP γ S did not significantly change the constant as compared with conventional mode (data not shown).

The voltage-dependence of steady-state inactivation was studied in a conventional manner. As the level of the conditioning pulses was shifted to the depolarizing direction, the magnitude of the inward currents decreased (Fig. 5A). The point of the half-maximum inactivation ($V_{1/2}$) was -79.8 ± 2.1 mV ($N=14$) in perforated mode (Fig. 5B). The $V_{1/2}$ in conventional mode shifted to hyperpolarizing direction (-86.3 ± 2.0 mV, $N=12$, $P < 0.05$). Internal 1 mmol l^{-1} GDP β S did not affect the $V_{1/2}$ (-86.1 ± 3.0 mV, $N=7$) as compared with conventional mode, but internal 0.5 mmol l^{-1} GTP γ S significantly shifted the $V_{1/2}$ to -98.4 ± 2.1 mV ($N=12$, $P < 0.05$; Fig. 5C).

The time course of recovery of the inward currents from inactivation was investigated using double-pulse protocol with varying pulse intervals. The two-step pulses (control and test pulse) were identical and consisted of a depolarization to -24 mV, lasting 20 ms (Fig. 6A). The time course of recovery was single exponential (Fig. 6B). The time constant was 9.6 ± 1.3 ms ($N=5$) in perforated mode and 13.1 ± 0.7 ms ($N=5$) in conventional mode, respectively. Addition of 0.5 mmol l^{-1} GTP γ S to the internal solution further prolonged the time constant to 16.5 ± 2.4 ms ($N=5$). Recovery was significantly more rapid in perforated mode than in conventional mode and the condition containing 0.5 mmol l^{-1} GTP γ S. However, there was no significant difference in the time constant between the conventional mode and after addition of GTP γ S.

Effects of cannabinoids on Na^+ current

In the present study, dialysis of GTP γ S into internal solution modulated activation and inactivation of Na^+ currents, suggesting regulation by a G protein-coupled mechanism. We therefore searched for the ligand that can modulate the Na^+ current activity. Parathyroid cells express the CaR and the PTH release from the cells is decreased by a CaR agonist, spermine (Quinn et al., 1997). Spermine (1 mmol l^{-1}), however, did not affect the Na^+ current activity (Fig. 7C). By contrast, beta-adrenergic agonists stimulate cAMP production and PTH release in parathyroid cells (Brown et al., 1977). Adrenaline ($10 \text{ } \mu\text{mol l}^{-1}$) also did not significantly inhibit the Na^+ current (Fig. 7C).

Although the cannabinoid receptors were not found on the cell membrane of parathyroid cells, frog parathyroid cells under perforated whole-cell mode were exposed to a putative endocannabinoid, 2-AG ether ($50 \text{ } \mu\text{mol l}^{-1}$). The drug did not change the basal properties of the cells, but reduced the Na^+ current. The peak current at -24 mV decreased to $36 \pm 8\%$ ($P < 0.05$) of the controls in 5 of 5 cells (Fig. 7C). Even when

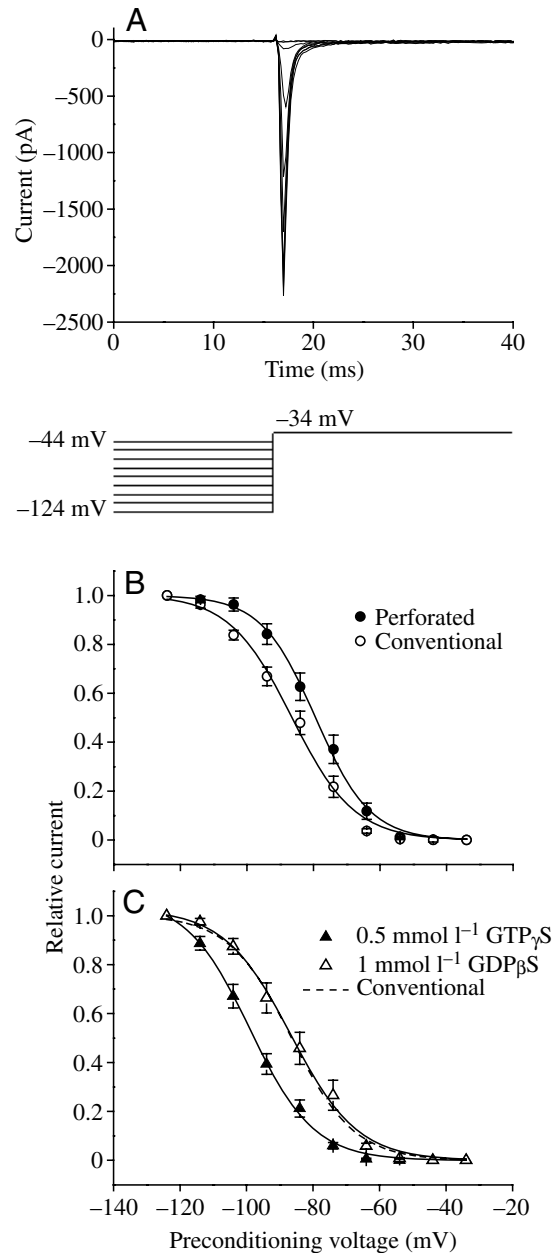


Fig. 5. Voltage dependence of steady-state inactivation of the Na^+ currents. (A) The dependence was determined by measuring peak current elicited by a single depolarization to -34 mV from a range of 200 ms conditioning voltages. (B) $V_{1/2} = -79.8$ mV, $k = 8.2$ mV for perforated recording (filled circles), $V_{1/2} = -86.3$ mV, $k = 9.4$ mV for conventional recording (open circles). (C) $V_{1/2} = -98.4$ mV, $k = 9.6$ mV for 0.5 mmol l^{-1} GTP γ S (filled triangles), $V_{1/2} = -86.1$ mV, $k = 10.0$ mV for 1 mmol l^{-1} GDP β S (open triangles). For comparison, the broken line for conventional recording is plotted in B. The values are means \pm S.E.M. obtained from 7–14 cells.

the external solution was returned to normal saline solution, the Na^+ current did not recover to the initial level. A cannabinomimetic aminoalkylindole, WIN 55,212-2 ($10 \text{ } \mu\text{mol l}^{-1}$) reversibly inhibited the Na^+ current (Fig. 7A,B).

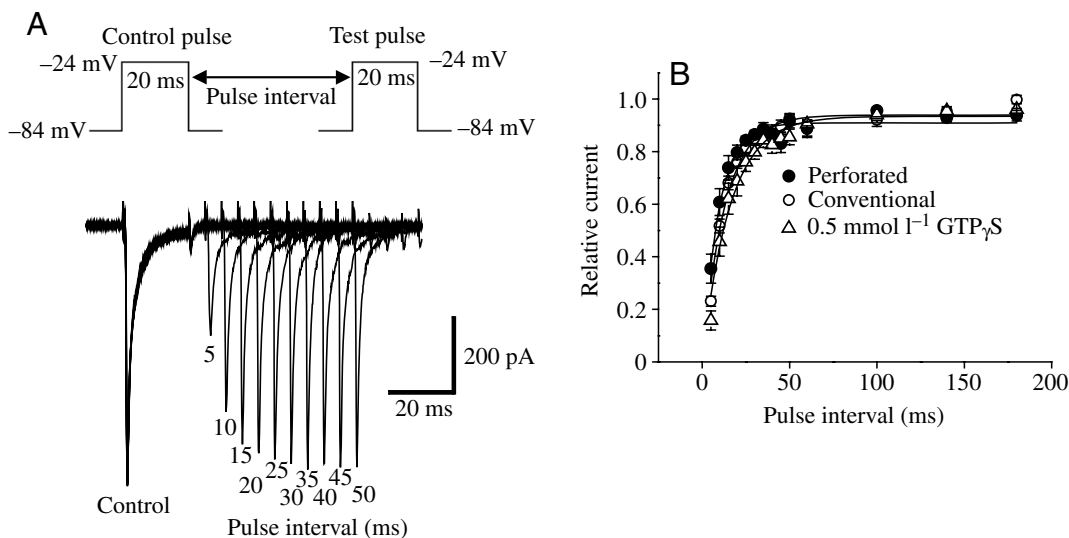


Fig. 6. Time course of recovery from inactivation. (A) Inward currents recorded using a double pulse protocol in which a 20 ms control pulse from -84 to -24 mV was followed by a second identical voltage pulse. (B) The plots show the recovery time course of the Na⁺ currents. The curves represent the fits of a single exponential function, giving values of time constants of 9.6 ± 1.2 ms ($N=5$) for perforated mode (filled circles), 13.1 ± 0.7 ms ($N=5$) in conventional mode (open circles) and 16.5 ± 2.4 ms ($N=5$) for the condition containing 0.5 mmol l^{-1} GTP γ S in the internal solution (open triangles).

The peak current at -24 mV decreased to $33 \pm 7\%$ ($N=5$, $P<0.05$) of the controls. WIN 55,212-2 shifted the $V_{1/2}$ of activation by 11.7 ± 1.6 mV ($N=4$, $P<0.05$; Fig. 8A,C) and the

$V_{1/2}$ of inactivation by 17.5 ± 1.9 mV ($N=4$, $P<0.05$; Fig. 8B,D). 2-AG ether also induced similar shift in the $V_{1/2}$ of activation and inactivation (Fig. 8C,D).

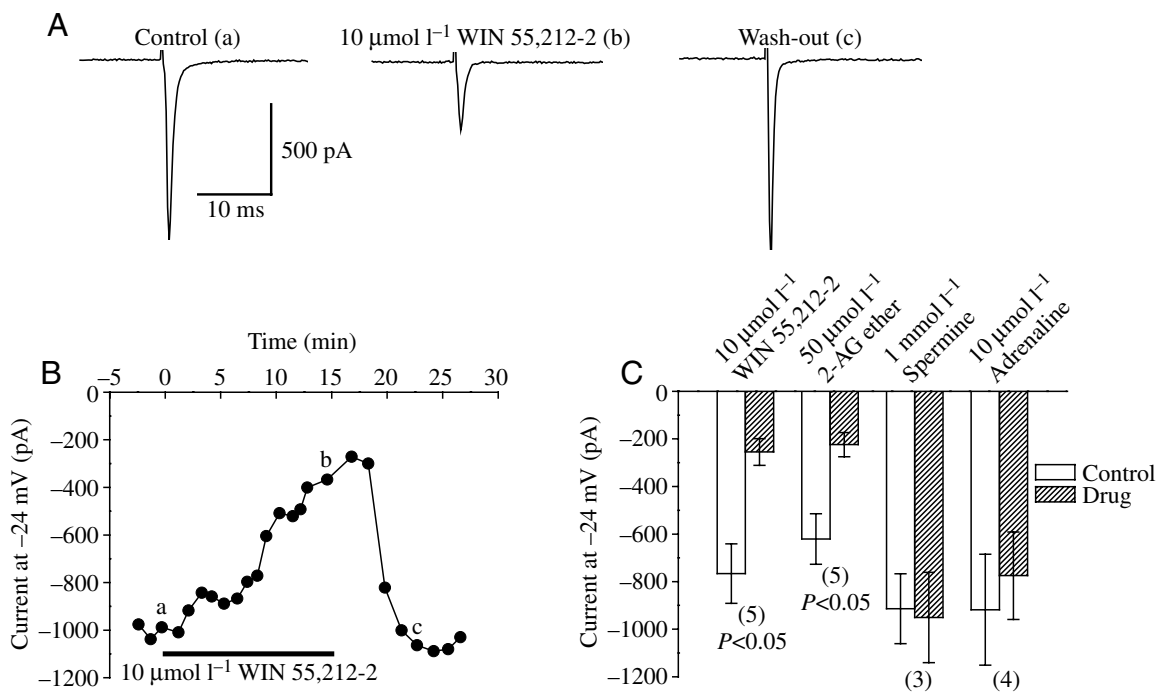


Fig. 7. Effects of WIN 55,212-2 and 2-AG ether on the Na⁺ currents. (A) Reversible inhibition of the Na⁺ current by $10 \mu\text{mol l}^{-1}$ WIN 55,212-2. The currents were elicited by a 20 ms pulse from a holding potential of -84 mV to a test potential of -24 mV. The current traces labelled a–c were obtained at the times indicated by the same letter on the time course. (B) Representative example of time course of the current signal. (C) Na⁺ current magnitudes before and after superfusion with each drug. Values are means \pm S.E.M. Numerals within parentheses are number of the cells sampled.

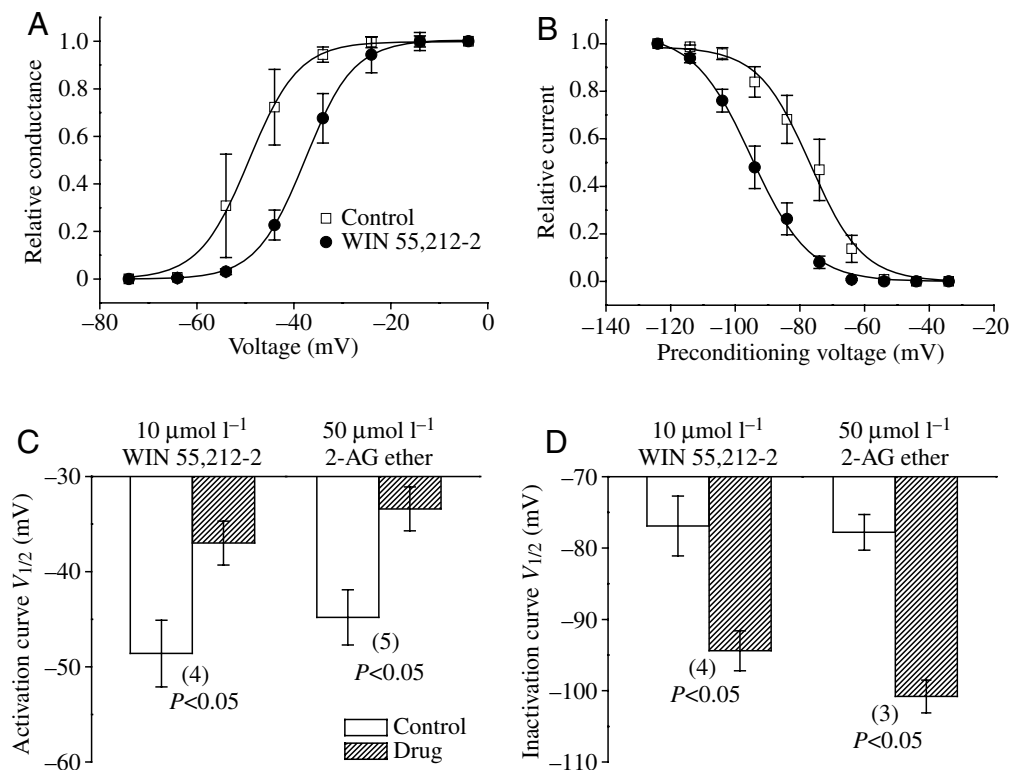


Fig. 8. Effects of WIN 55,212-2 and 2-AG ether on activation and inactivation of the Na^+ currents. (A) Voltage dependence of activation before and after superfusion with $10 \mu\text{mol l}^{-1}$ WIN 55,212-2. $V_{1/2} = -48.6 \text{ mV}$, $k = -5.1 \text{ mV}$ for control (open squares), $V_{1/2} = -37.0 \text{ mV}$, $k = -5.0 \text{ mV}$ for WIN 55,212-2 (filled circles). (B) Voltage dependence of inactivation before and after superfusion with $10 \mu\text{mol l}^{-1}$ WIN 55,212-2 (filled circles). $V_{1/2} = -76.9 \text{ mV}$, $k = 8.1 \text{ mV}$ for control (open squares), $V_{1/2} = -94.4 \text{ mV}$, $k = 9.0 \text{ mV}$ for WIN 55,212-2. (C) $V_{1/2}$ of activation before (white bars) and after superfusion with each drug (hatched bars). (D) $V_{1/2}$ of inactivation before (white bars) and after superfusion with each drug (hatched bars). Values are means \pm S.E.M. Numerals within parentheses are number of the cells sampled.

Effects of protein kinases on the Na^+ current

The cytoplasmic loop in the Na^+ channels possesses several protein kinase A (PKA) and protein kinase C (PKC) phosphorylation sites (Cantrell et al., 2003). To determine the role of PKC on Na^+ current, we tested the effect of a PKC activator, PDBu on the properties of Na^+ current. PDBu ($10 \mu\text{mol l}^{-1}$) decreased the Na^+ current at -24 mV to $37 \pm 8\%$ of the controls (Fig. 9C). A wash-out with normal saline solution was not observed (Fig. 9A). PDBu did not significantly shift the $V_{1/2}$ of activation (Fig. 10A), but induced the hyperpolarizing shift of $11.9 \pm 2.6 \text{ mV}$ ($N=5$, $P < 0.05$) in the $V_{1/2}$ of inactivation (Fig. 10B). An adenylyl cyclase activator, forskolin ($10 \mu\text{mol l}^{-1}$) did not significantly inhibit the Na^+ current (Fig. 9C).

We further evaluated the effect of a PKC inhibitor (chelerythrine) on the modulation of Na^+ current elicited by cannabinoids. Chelerythrine ($10 \mu\text{mol l}^{-1}$) itself did not affect the Na^+ current (Fig. 11A). Even when frog parathyroid cells were pre-incubated for 10 min in a solution containing $10 \mu\text{mol l}^{-1}$ chelerythrine, subsequent application of $10 \mu\text{mol l}^{-1}$ WIN 55,212-2 still inhibited the Na^+ currents (Fig. 11A,B). Furthermore, in the presence of PKC inhibitor, WIN 55,212-2 shifted the $V_{1/2}$ of activation by $11.3 \pm 2.6 \text{ mV}$

($N=3$, $P < 0.05$; Fig. 11C) and the $V_{1/2}$ of inactivation by $18.3 \pm 5.0 \text{ mV}$ ($N=3$, $P < 0.05$; Fig. 11D). These results indicate that WIN 55,212-2 acts on the Na^+ currents, probably through a mechanism independent of PKC.

Discussion

The present study shows that frog parathyroid cells express TTX-sensitive voltage-gated Na^+ channels in the cell membrane. However, most Na^+ channels were silent at resting potential (-30 mV). The silent Na^+ channels in the parathyroid cells could only be restored if a hyperpolarizing voltage was applied. Similarly, rat gonadotropes in the anterior lobe of the pituitary glands fire action potentials at the termination of the hyperpolarization elicited by gonadotropin-releasing hormone (GnRH; Tse and Hille, 1993); in these cells, fast depolarizations in action potentials open voltage-gated Ca^{2+} channels that allow entry of extracellular Ca^{2+} . Nevertheless, in the present experiments, the $V_{1/2}$ for inactivation was about -80 mV in perforated mode, and few cells that possess such a deep resting potential are excitable.

By comparing the activation and inactivation processes in the presence and absence of $\text{GTP}\gamma\text{S}$, we observed evidence

that the activation and inactivation of Na^+ currents are regulated by guanine nucleotides, perhaps as a G protein-coupled mechanism. In the absence (conventional) of $\text{GTP}\gamma\text{S}$, the mean $V_{1/2}$ for Na^+ current activation was about -46 mV. A similar mean value was observed in the presence of $\text{GDP}\beta\text{S}$ in the pipette solution. Since internal $\text{GTP}\gamma\text{S}$ shifted the $V_{1/2}$ to a

more positive level (-36 mV), the presence of $\text{GTP}\gamma\text{S}$ results in the activation of a G protein-dependent mechanism, which may be functionally important in regulating Na^+ current activation. A similar effect of $\text{GTP}\gamma\text{S}$ was also observed in the inactivation process. Our results suggest that a G protein-dependent inhibitory mechanism may be involved in both activation and inactivation processes in the voltage-gated Na^+ channels of frog parathyroid cells. Furthermore, in perforated mode, the $V_{1/2}$ for inactivation shifted to a more positive value than in conventional mode. This also suggests that the Na^+ channels may be regulated by another enhancing mechanism. It has been reported that voltage-gated Na^+ channels are under the regulation of G proteins. In rat cardiac myocytes, internal $\text{GTP}\gamma\text{S}$ inhibits the Na^+ channel by shifting the steady-state inactivation to more negative potentials (Schubert et al., 1989 and 1990). In contrast, $\text{GTP}\gamma\text{S}$ enhances Na^+ current in frog olfactory receptor neurons (Pun et al., 1994).

Two types (CB_1 and CB_2) of cannabinoid receptors have been cloned from many vertebrates including mammals, birds, amphibians and fish (Lutz, 2002). CB_1 is expressed predominantly in the central and peripheral nervous system,

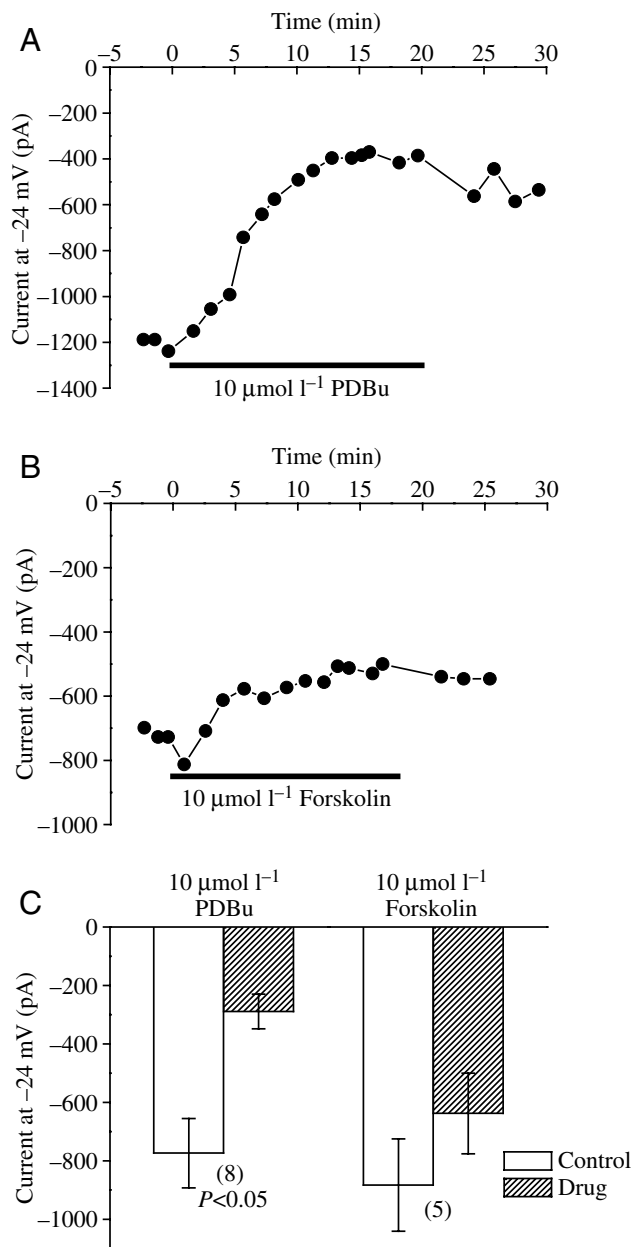


Fig. 9. Effects of PDBu and forskolin on the Na^+ currents. (A) Representative example of time course of the current signal after superfusion with $10 \mu\text{mol l}^{-1}$ PDBu. (B) Representative example of time course of the current signal after superfusion with $10 \mu\text{mol l}^{-1}$ forskolin. (C) Na^+ current magnitude before (white bars) and after superfusion with each drug (hatched bars). The currents were elicited by 20 ms pulse from a holding potential of -84 mV to a test potential of -24 mV. Values are means \pm S.E.M. Numerals within parentheses are number of the cells sampled.

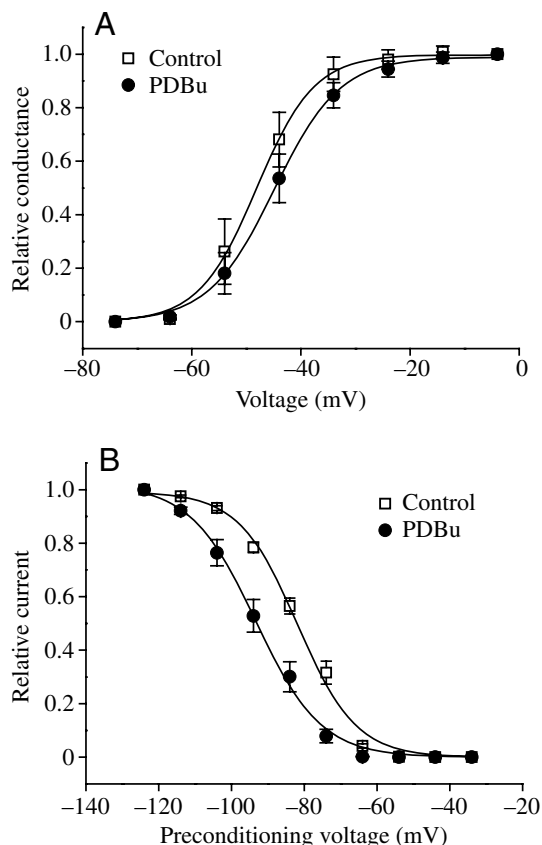


Fig. 10. Effect of $10 \mu\text{mol l}^{-1}$ PDBu on activation and inactivation of the Na^+ currents. (A) Voltage dependence of activation. $V_{1/2} = -47.7$ mV, $k = -5.3$ mV for control (open squares), $V_{1/2} = -44.3$ mV, $k = -6.0$ mV for PDBu (filled circles). (B) Voltage dependence of inactivation. $V_{1/2} = -81.8$ mV, $k = 8.1$ for control (open squares), $V_{1/2} = -93.7$ mV, $k = 9.0$ mV for PDBu (filled circles). Values are mean \pm S.E.M. obtained from 5–8 cells.

while CB_2 is present exclusively in immune cells. CB_1 is a typical $G_{i/o}$ -coupled receptor and can initiate various signaling events (Piomelli, 2003). These include closure and opening of ion channels, inhibition of adenylyl cyclase activity and stimulation of protein kinases. In the present study we demonstrate that external application of a putative endocannabinoid, 2-AG ether, and cannabinomimetic aminoalkylindole WIN 55,212-2, produced potent inhibition of the voltage-gated Na^+ current in frog parathyroid cells, although their receptors are not found on the cells. External cannabinoids as well as internal $GTP\gamma S$ shifted the $V_{1/2}$ for activation and inactivation, suggesting that cannabinoids could inhibit the Na^+ current *via* a G protein-dependent mechanism. Although a PKC activator, PDBu, also inhibited the Na^+ current and shifted the $V_{1/2}$ for inactivation, the modulating effect of cannabinoids on the Na^+ current cannot be explained by PKC activity. Further studies will be required to elucidate the mechanism for modulation induced by cannabinoids.

In conventional whole-cell configuration, human parathyroid cells hardly displayed macroscopic K^+ current in low intracellular Ca^{2+} concentration ($<10 \text{ nmol l}^{-1}$; Välimäki

et al., 2003). We also could not record voltage-gated outward currents in response to the depolarizing voltage steps from a holding potential of -84 mV . The free Ca^{2+} concentration of the present internal solution is calculated to be about 16 nmol l^{-1} using the Webmaxc software. As expected from those results, both human and frog parathyroid cells displayed low resting potential in the condition of low intracellular Ca^{2+} . In human parathyroid cells, the K^+ current increases and the membrane potentials are hyperpolarized when extracellular Ca^{2+} concentration is elevated (Välimäki et al., 2003). On the other hand, high extracellular Ca^{2+} elicits Ca^{2+} -activated Cl^- conductance in frog parathyroid cells (Okada et al., 2001). The activation of Cl^- conductance may hyperpolarize the cells if intracellular Cl^- concentration is low. Further experiments should clarify more fully the relationships between changes in extracellular Ca^{2+} concentration and the regulation of Ca^{2+} -activated Cl^- channel in frog parathyroid cells.

In conclusion, frog parathyroid cells possess voltage-gated Na^+ channels whose activity may be modulated by cannabinoids.

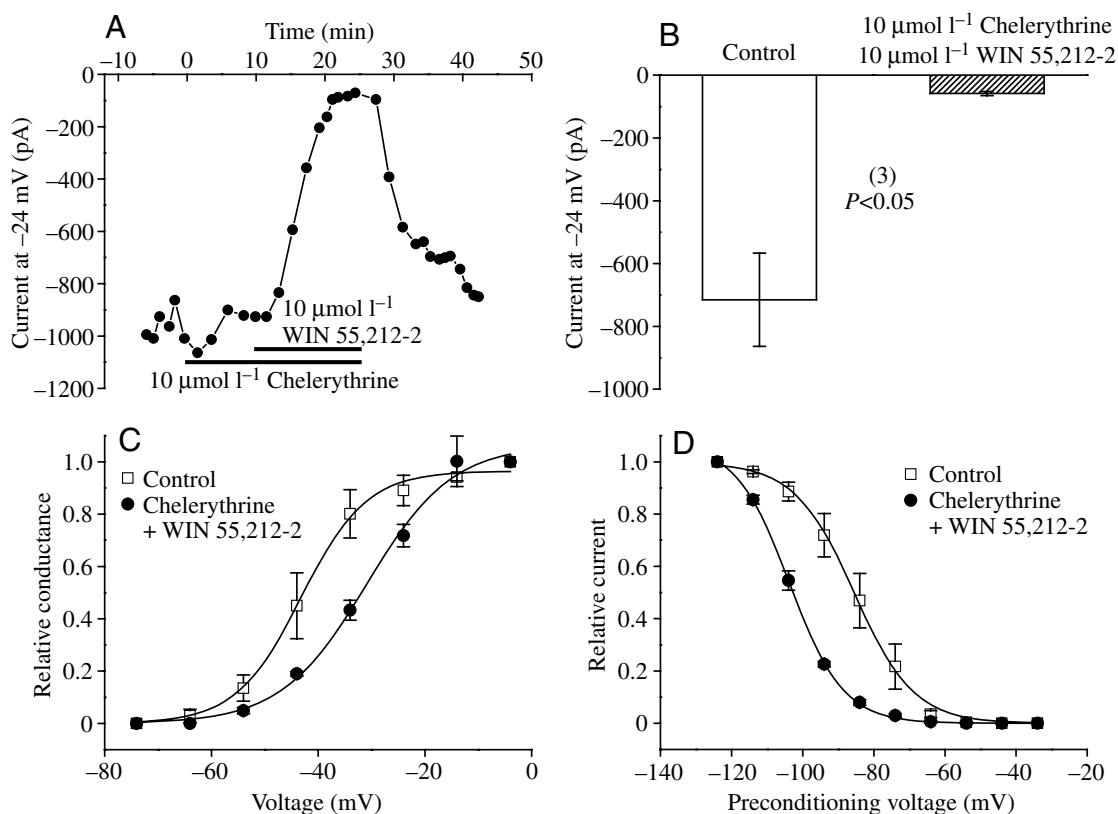


Fig. 11. Effect of WIN 55,212-2 on the Na^+ currents in the presence of an inhibitor of PKC. (A) Representative example of time course of the current signal. The currents were elicited by a pulse from a holding potential of -84 mV to a test potential of -24 mV . (B) Mean values of Na^+ current magnitudes before (white bar) and after superfusion with $10 \mu\text{mol l}^{-1}$ chelerythrine and $10 \mu\text{mol l}^{-1}$ WIN 55,212-2 (hatched bar). Numerals within parentheses are number of the cells sampled. (C) Voltage dependence of activation. $V_{1/2} = -42.0 \text{ mV}$, $k = -6.1 \text{ mV}$ for control (open squares), $V_{1/2} = -30.7 \text{ mV}$, $k = -8.0 \text{ mV}$ for chelerythrine plus WIN 55,212-2 (filled circles). (D) Voltage dependence of inactivation. $V_{1/2} = -83.5 \text{ mV}$, $k = 8.4 \text{ mV}$ for control (open squares), $V_{1/2} = -103.8 \text{ mV}$, $k = 7.6 \text{ mV}$ for chelerythrine plus WIN 55,212-2 (filled circles). The values are mean \pm S.E.M. obtained from three cells.

List of symbols and abbreviations

| | |
|--------------------------------------|---|
| 2-AG | 2-arachidonoylglycerol |
| [Ca ²⁺] _o | extracellular free Ca ²⁺ concentration |
| 1,25(OH) ₂ D ₃ | 1,25-dihydroxycholecalciferol |
| <i>a</i> | maximum magnitude |
| CaR | Ca ²⁺ -sensing receptor |
| CT | calcitonin |
| DMSO | dimethyl sulphoxide |
| <i>G</i> | peak conductance |
| GPCR | G protein-coupled receptor |
| <i>I</i> | current |
| <i>k</i> | Boltzmann slope factor |
| PKA | protein kinase A |
| PKC | protein kinase C |
| PTH | parathyroid hormone |
| <i>t</i> | time |
| <i>V</i> | voltage |
| <i>V</i> _{rev} | apparent reversal potential |
| <i>τ</i> | time constant |

This work was supported by Grants-in-Aid (14540630) from Japan Society for the Promotion of Science to Y.O.

References

- Brown, E. M., Hurwitz, S. and Aurbach, G. D.** (1977). Beta-adrenergic stimulation of cyclic AMP content and parathyroid hormone release from isolated bovine parathyroid cells. *Endocrinology* **100**, 1696-1702.
- Brown, E. M., Gamba, G., Riccardi, D., Lombardi, M., Butters, R., Kifor, O., Sun, A., Hediger, M. A., Lytton, J. and Hebert, S. C.** (1993). Cloning and characterization of an extracellular Ca²⁺-sensing receptor from bovine parathyroid. *Nature* **366**, 575-580.
- Bruce, B. R. and Anderson, N. C., Jr** (1979). Hyperpolarization in mouse parathyroid cells by low calcium. *Am. J. Physiol.* **236**, C15-C21.
- Cantrell, A. R., Tibbs, V. C., Yu, F. H., Murphy, B. J., Sharp, E. M., Qu, Y., Catterall, W. A. and Scheuer, T.** (2002). Molecular mechanism of convergent regulation of brain Na⁺ channels by protein kinase C and protein kinase A anchored to AKAP-15. *Mol. Cell. Neurosci.* **21**, 63-80.
- Castellano, A., Pintado, E. and López-Barneo, J.** (1987). Ca²⁺- and voltage-dependent K⁺ conductance in dispersed parathyroid cells. *Cell Calcium* **8**, 377-383.
- Chang, W., Pratt, S. A., Chen, T. H., Tu, C. L., Mikala, G., Schwartz, A. and Shoback, D.** (2001). Parathyroid cells express dihydropyridine-sensitive cation current and L-type calcium channel subunits. *Am. J. Physiol.* **281**, E180-E189.
- Dascal, N.** (2001). Ion-channel regulation by G proteins. *Trends Endocrinol. Metab.* **12**, 391-398.
- Hamill, O. P., Marty, A., Neher, E., Sakmann, B. and Sigworth, F. J.** (1981). Improved patch-clamp techniques for high-resolution current recording from cells and cell-free membrane patches. *Pflügers Arch.* **391**, 85-100.
- Hofer, A. M. and Brown, E. M.** (2003). Extracellular calcium sensing and signalling. *Nat. Rev. Mol. Cell. Biol.* **14**, 530-538.
- Jia, M., Ehrenstein, G. and Iwasa, K.** (1988). Unusual calcium-activated potassium channels of bovine parathyroid cells. *Proc. Natl. Acad. Sci. USA* **85**, 7236-7239.
- Kanazirska, M. P., Vassilev, P. M., Ye, C. P., Francis, J. E. and Brown, E. M.** (1995). Intracellular Ca²⁺-activated K⁺ channels modulated by variations in extracellular Ca²⁺ in dispersed bovine parathyroid cells. *Endocrinology* **136**, 2238-2243.
- Komwatana, P., Conigrave, A. D., Delbridge, L., Young, J. A. and Cook, D. I.** (1994). Intracellular Ca²⁺ inactivates an outwardly rectifying K⁺ current in human adenomatous parathyroid cells. *Pflügers Arch.* **426**, 320-327.
- López-Barneo, J. and Armstrong, C. M.** (1983). Depolarizing response of rat parathyroid cells to divalent cations. *J. Gen. Physiol.* **82**, 269-294.
- Lutz, B.** (2002). Molecular biology of cannabinoid receptors. *Prostaglandins Leukot. Essent. Fatty Acids* **66**, 123-142.
- McHenry, C. R., Stenger, D. B. and Kunze, D. L.** (1998). Inwardly rectifying K⁺ channels in dispersed bovine parathyroid cells. *J. Surg. Res.* **76**, 37-40.
- Okada, Y., Miyamoto, T., Toda, K., Miyazaki, T. and Hotokezaka, H.** (2001). Extracellular calcium-induced response in frog parathyroid cells. *Zool. Sci.* **18**, S115.
- Piomelli, D.** (2003). The molecular logic of endocannabinoid signaling. *Nat. Rev. Neurosci.* **4**, 873-884.
- Pun, R. Y., Kleene, S. J. and Gesteland, R. C.** (1994). Guanine nucleotides modulate steady-state inactivation of voltage-gated sodium channels in frog olfactory receptor neurons. *J. Membr. Biol.* **142**, 103-111.
- Quinn, S. J., Ye, C. P., Diaz, R., Kifor, O., Bai, M., Vassilev, P. and Brown, E.** (1997). The Ca²⁺-sensing receptor: a target for polyamines. *Am. J. Physiol.* **273**, C1315-C1323.
- Rae, J., Cooper, K., Gates, P. and Watsky, M.** (1991). Low access resistance perforated patch recordings using amphotericin B. *J. Neurosci. Methods* **37**, 15-26.
- Sand, O., Ozawa, S. and Hove, K.** (1981). Electrophysiology of cultured parathyroid cells from the goat. *Acta Physiol. Scand.* **113**, 45-50.
- Sasayama, Y. and Oguro, C.** (1974). Notes on the topograph and morphology of the parathyroid glands in some Japanese anurans. *Annot. Zool. Japon.* **47**, 232-238.
- Schubert, B., Vandongen, A. M., Kirsch, G. E. and Brown, A. M.** (1989). Beta-adrenergic inhibition of cardiac sodium channels by dual G-protein pathways. *Science* **245**, 516-519.
- Schubert, B., Vandongen, A. M., Kirsch, G. E. and Brown, A. M.** (1990). Inhibition of cardiac Na⁺ currents by isoproterenol. *Am. J. Physiol.* **258**, H977-H982.
- Tse, A. and Hille, B.** (1993). Role of voltage-gated Na⁺ and Ca²⁺ channels in gonadotropin-releasing hormone-induced membrane potential changes in identified rat gonadotropes. *Endocrinology* **132**, 1475-1481.
- Välimäki, S., Höög, A., Larsson, C., Farnebo, L. O. and Bränström, R.** (2003). High extracellular Ca²⁺ hyperpolarizes human parathyroid cells via Ca²⁺-activated K⁺ channels. *J. Biol. Chem.* **278**, 49685-49690.
- Wickman, K. and Clapham, D. E.** (1995). Ion channel regulation by G proteins. *Physiol. Rev.* **75**, 865-885.